Int. J. Radiation Oncology Biol. Phys., Vol. 15, pp. 1209–1218
Printed in the U.S.A.

0360-3016/88 $3.00 + .00

● *Original Contribution*

THERMAL DISTRIBUTION STUDIES OF HELICAL COIL MICROWAVE ANTENNAS FOR INTERSTITIAL HYPERTHERMIA

TORU SATOH, M.D., PAUL R. STAUFFER, M.S.E.E. AND JOHN R. FIKE, PH.D.

Brain Tumor Research Center of the Department of Neurological Surgery, and Department of Radiation Oncology, School of Medicine, University of California, San Francisco, CA

An implantable 915 MHz helical coil antenna was developed for improved localization and control of interstitial microwave hyperthermia. The radiating element consisted of a fine wire coil wound back over the inner conductor of a miniature semi-rigid coaxial cable in place of the terminal portion of outer conductor. The power deposition profiles from single helical coil antennas were studied both in homogeneous phantom and in muscle tissue *in vivo* and compared to those of single half-wavelength linear dipole antennas. The effects of variable coil length, turn density, and antenna insertion depth in tissue were characterized. The helical coil antennas produced a well-localized heating pattern with a sharp falloff of temperature in both directions axially from the coil element. One of the best heating patterns was obtained with a 35 turn, 35 mm long helical coil element which was separated from the antenna feedline outer conductor by a 1 mm gap (HCS-35(1)/36). This antenna showed a marked shift of the effectively heated volume toward the antenna tip and essentially no dependence of the heating pattern on insertion depth. In contrast, the axial power deposition profiles of dipole antennas were strongly affected by insertion depth and exhibited an inadequately heated area at the antenna tip even with $\frac{1}{2}$–$\frac{3}{4}$ wavelength insertion. Thermal distribution studies showed that the single helical coil microwave antenna provided more predictable, well-localized heating of deep-seated tissues, with minimal requirement for over-implanting of the treatment volume.

Hyperthermia, Interstitial hyperthermia, Microwave antenna, Thermal dosimetry.

INTRODUCTION

Many recent laboratory and clinical trials have demonstrated the efficacy of combining interstitial hyperthermia with interstitial radiation therapy.[2,3,8,10–12] Invasive half-wavelength dipole microwave antennas have been used to induce localized thermal fields within specific tissue volumes by inserting them into the same afterloading plastic catheters used for the brachyradiotherapy procedure. This combination has shown more effective tumor response than either of the treatment modalities alone.[2,3,11,12] There are, however, three major problems that limit the applicability and effectiveness of standard dipole microwave antennas for interstitial hyperthermia:[4,14,15] (a) variability of heating profile with different insertion depths in tissue; (b) restricted range of possible heating lengths for a given microwave frequency; and (c) inadequately heated "dead length" or "cold area" at the antenna tip.

In an effort to minimize these problems and to provide a reproducible heating pattern for wider application to the variety of tumor volumes and locations, we developed and characterized a new configuration of an implantable helical coil microwave antenna. The present investigation defines the thermal profiles induced by these helical coil antennas both in phantom and in muscle tissue *in vivo*, and compares them to the thermal profiles produced by standard half-wavelength dipole antennas.

METHODS AND MATERIALS

Antenna design

Helical coils for the antennas were made by wrapping a 0.32 mm diameter wire around a stainless steel wire form according to the desired coil length and turn density. Antennas were constructed by removing a length of

This paper was presented at the 8th Annual Meeting of the North American Hyperthermia Group, Atlanta, GA, February, 1987.

Reprint requests to: Paul R. Stauffer, M.S.E.E., Hyperthermia Section of the Department of Radiation Oncology, Box 0226, University of California, San Francisco, CA 94143.

Acknowledgement—We would like to thank Ms. Theresa M. Seilhan for her careful and able assistance in the *in vivo* animal studies. This work was supported in part by NIH grants CA-39428 and CA-13525.

Accepted for publication 18 May 1988.

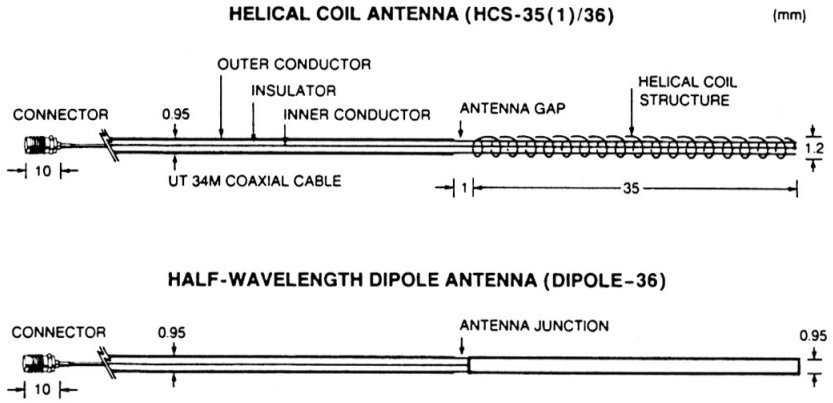

Fig. 1. Schema showing the dimensions and configurations of the implantable microwave antennas. A helical coil-separated antenna (above) with 35 turns per 35 mm coil length with a 1 mm gap (HCS-35(1)/36), and a typical half-wavelength dipole antenna below (Dipole-36).

the outer conductor from a 0.95 mm O.D. miniature semi-rigid coaxial cable* and sliding the fine wire coil around the inner conductor insulator (0.61 mm O.D.). The helical coil was soldered to the distal end of the inner conductor leaving a 1 mm wide "gap" between the proximal end of the coil and the outer conductor. Because of the connection configuration of the helical coil to the feedline, these antennas were called helical coil-separated (HCS) antennas [14]. Several variations of HCS antennas were made and were described in terms of the number of coil turns per bare insulated inner conductor length (mm), with the gap width in parenthesis (mm): HCS-25(1)/36, HCS-50(1)/51, etc. (Fig. 1). The outer diameter of each antenna, including the helical coil portion, was less than 1.2 mm so that the entire assembly could be inserted into a 16-guage (1.23 mm I.D.) plastic catheter. Commercially available half-wavelength dipole antennas (0.95 mm O.D.) with 35 mm active radiator length distal to the 1 mm spaced "junction" (Dipole-36)† were used for comparison with the helical coil antennas.

Phantom experiments

Single antenna power deposition profiles of the different antenna types were studied in a muscle tissue phantom which was a mixture of distilled water (75.15%), TX-150 (8.42%), sodium chloride (0.996%), and polyethylene powder (15.44%).[1] This material was contained in a $10 \times 10 \times 25$ cm plexiglass box traversed by arrays of parallel 16-gauge plastic catheters for the single antennas and the optical fiber thermometry probes.‡

The effects of helical coil length on the axial power deposition profiles were investigated using antennas with different lengths, each with 10 turns per 10 mm: HCS-30(1)/31, HCS-40(1)/41, and HCS-50(1)/51. The effects of turn density were investigated using 35 mm long helical coil antennas with either 7, 10, or 16 turns per 10 mm: HCS-25(1)/36, HCS-35(1)/36, and HCS-56(1)/36. The influence of antenna insertion depth on the power deposition profiles was studied using HCS-35(1)/36 and Dipole-3.6 antennas inserted either 4.5, 7.0, or 10.5 cm below the tissue surface. Additionally, HCS antennas were tested with an insertion depth shorter than the total coil length (1.5 cm out of 3.5 cm coil length).

Each antenna was driven at 915 MHz using a continuous wave power source.‡ While the antennas were adequately matched alone (typically -8 dB $\{-10$ dB$\}$ return loss or voltage standing wave ratio ≤ 2.3 $\{\leq 1.9\}$ respectively for the helical coil {dipole} antennas), precise electrical matching of the antennas to the generator and feedline was accomplished using a double stub tuner§ for accurate power monitoring and control. Multiple-sensor optical fiber probes (1 mm O.D.) with four sensors spaced 0.5–1 cm apart were inserted from both sides of the phantom into a catheter which was parallel to and 0.5 cm away from the antenna (r = 5 mm catheter). All temperature and power information was recorded by the data acquisition system‡ every 10 seconds. Repeated 20-Watt, 30-second heat trials were used to determine the specific absorption rate (SAR) at 0.5–1 cm intervals along the r = 5 mm catheter. The single antenna power deposition profiles were determined by first normalizing the SAR of each point to the maximum SAR of its linear distribution (normalized SAR profile). The normalized r = 5 mm profiles of each antenna were obtained at several different phantom locations and then averaged together. To reduce errors from specific antenna construction and phantom variations, at least two antennas of each configuration were tested in two or more phantom mixtures.

Several parameters (Fig. 2) derived from the r = 5 mm axial power deposition profiles were used to quantify an-

* UT-34M, Uniform Tubes, Inc., Collegeville, PA.

† Interstitial microwave antenna, Clini-Therm Corporation, Dallas, TX.

‡ Mark-VI or IX, Clini-Therm Corporation, Dallas, TX.

§ No. 1729, Maury Microwave, Cucamonga, CA.

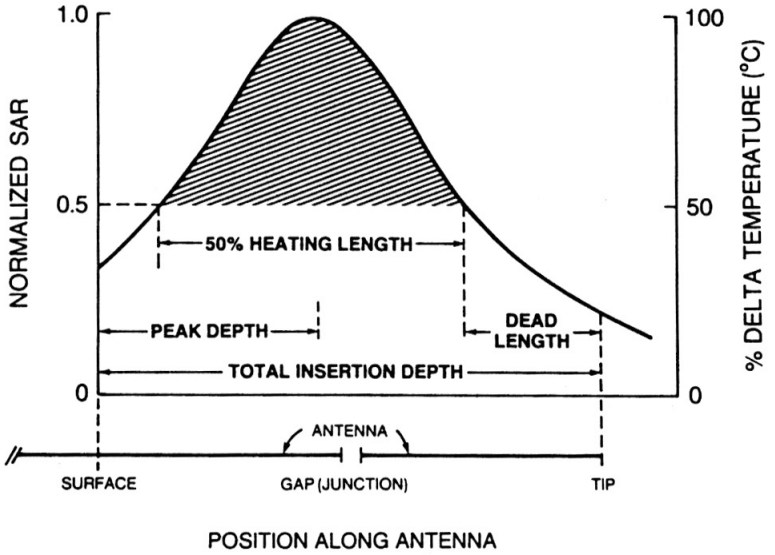

Fig. 2. Schema showing the parameters used for the comparative evaluation of r = 5 mm axial power deposition profiles. **Peak depth** defines the location of the temperature peak relative to the tissue surface. The **50% HL** quantifies the total length along the antenna axis heated above 50% of the maximum temperature rise in the profile. **Dead length** refers to that portion of the profile adjacent to the antenna tip which is heated to less than 50% of the maximum temperature rise.

tenna heating effectiveness:[14] (a) uniformity of heating as determined by the length of tissue in cm heated above 50% of the maximum temperature rise (**50% HL**); (b) location of the temperature peak relative to the phantom surface (**Peak Depth**); and (c) length of phantom material toward the end of the antenna which showed less than 50% of the maximum temperature rise (**Dead Length**).

In vivo *experiments*

The axial and radial power deposition profiles of HCS-35(1)/36 and Dipole-36 antennas were studied in dog thigh muscle. Repeated heating experiments in the same implant site[16–18] were used to compare the temperature profiles from each antenna design.

Experiments were performed in 15 implant sites in four adult mongrel dogs. Each dog was premedicated with atropine sulfate and acepromazine maleate, induced with 4% sodium thiamylal, and maintained at a surgical level of anesthesia with 1.0% methoxyflurane in oxygen. Four trocars were inserted in the muscle through the skin via a 1.8 cm thick plexiglass template. Three parallel trocars spaced 0.5 cm apart entered through the skin to a depth of either 4.5, 7.0, or 10.5 cm from the surface. Using a second template attached at a right angle to the first, an additional trocar was placed perpendicular to and just touching the others in the plane of the antenna gap or junction. Closed-end 16-gauge plastic catheters were inserted and the metal trocars withdrawn. A single antenna was placed into the central catheter. A multisensor thermometry probe with four sensors spaced 1 cm apart was placed on one side of the antenna for the axial profile, and a single-sensor probe (0.7 mm O.D.) was inserted into the catheter on the other side for the power

Table 1. Antenna heating characteristics in phantom

Antenna type	No. of trials	Insertion depth (cm)	Peak depth (cm)	50% HL (cm)	Dead length (cm)	Max SAR (W/kg/W)
HCS-30(1)/31	13	7.0	6.0	3.5	0.0	12.3
HCS-40(1)/41	15	7.0	6.0	4.4	0.0	8.9
HCS-50(1)/51	8	7.0	5.0	5.2	0.1	8.2
HCS-25(1)/36	12	7.0	6.0	3.5	−0.2	11.0
HCS-35(1)/36*	16	7.0	6.0	4.0	−0.2	11.5
HCS-56(1)/36	12	7.0	6.0	3.7	0.0	14.5
DIPOLE-36*	20	7.0	3.0	4.4	1.9	12.1

Note: Negative values of dead length represent an extension of the 50% heating length beyond the antenna tip. See Figure 2 and text for an explanation of the heating parameters obtained from the r = 5 mm axial power deposition profiles: Peak depth, 50% HL, Dead length. Max SAR represents the maximum SAR (W/kg/W) obtained at the peak of each profile.

* These data are duplicated in Table 2.

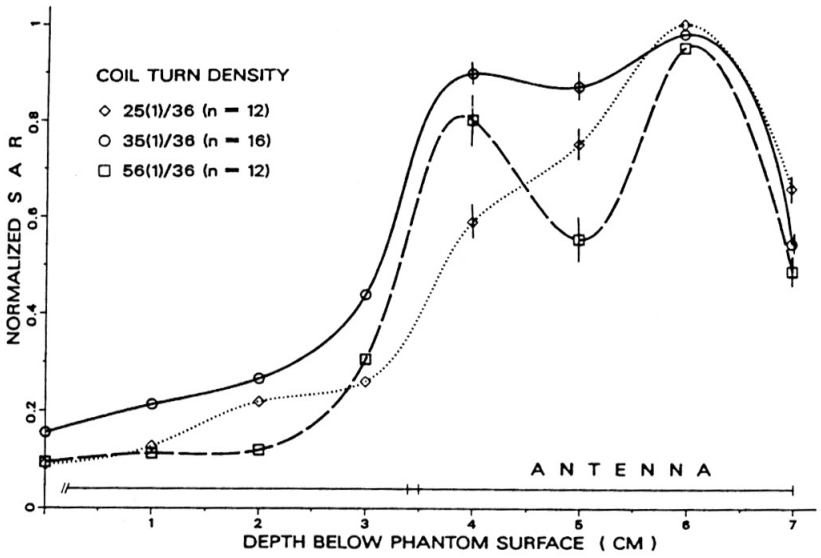

Fig. 3. Effects of helical coil turn density on the axial direction power deposition profiles. The 35 mm long helical coil antennas with either 7, 10, or 16 turns per 10 mm; HCS-25(1)/36, HCS-35(1)/36, and HCS-56(1)/36 were compared in 12-16 independent heat trials in two tissue equivalent phantom models. Note the nearly identical peak depths and 50% HL's but significantly different shape of the peak shoulders.

control. Radial thermal profiles were obtained with a second 1 cm spacing multi-sensor probe inside the perpendicular catheter. Using 3–5 Watts at 915 MHz, a relatively stable temperature distribution around the antenna was achieved within 10 minutes, and was maintained for another 10–15 minutes in each trial for temperature mapping. The stationary single-sensor probe was used for computerized temperature feedback control to maintain a constant temperature differential above baseline (Delta-T) of 5–7°C at the peak of the axial (r = 5 mm) profile throughout and between individual trials. Temperature distributions in the axial and radial directions were recorded by mapping the multi-sensor probes in 2 or 5 mm increments. Comparative trials with the other antennas followed a 30-minute break to allow the tissue to return to initial temperature conditions. The order of antenna trials was varied in the different implant sites, and results averaged to reduce the effect of the antenna test sequence. Additionally, care was taken not to exceed 44–45°C maximum tissue temperature or 25-minute heating periods to avoid significant alteration of tissue properties which might affect the induced temperature distributions.[16–18] To compare temperature profiles obtained in different animal implant sites with varying initial temperature conditions, Delta-T's were calculated for each measured point, and were normalized to a percentage of the maximum Delta-T of each r = 5 mm distribution (% Delta-Temperature profile). These normalized profiles were then averaged together to reduce the distribution perturbing effects of tissue inhomogeneities, and variable initial temperature conditions. Comparative thermal profile studies were always performed with an equal number of trials for each antenna in each implant site.

RESULTS

Phantom experiments

In the series of experiments using a constant 7 cm insertion depth, the heating volume of 3–5 cm long helical

Table 2. Antenna heating characteristics vs. antenna insertion depth in phantom

Antenna type	No. of trials	Insertion depth (cm)	Peak depth (cm)	50% HL (cm)	Dead length (cm)	Max SAR (W/kg/W)
HCS-35(1)/36	20	1.5*	1.0	1.3	−0.2	10.1
	10	4.5	4.0	4.2	−0.4	11.3
	16	7.0	6.0	4.0	−0.2	11.5
	16	10.5	10.0	4.4	−0.4	11.8
DIPOLE-36	12	4.5	1.0	3.8	0.7	12.5
	20	7.0	3.0	4.4	1.9	12.1
	16	10.5	7.0	6.2	1.7	11.7

See Table 1 for an explanation of the parameters.
* No equivalent test was possible for the Dipole-36 with 1.5 cm total insertion depth.

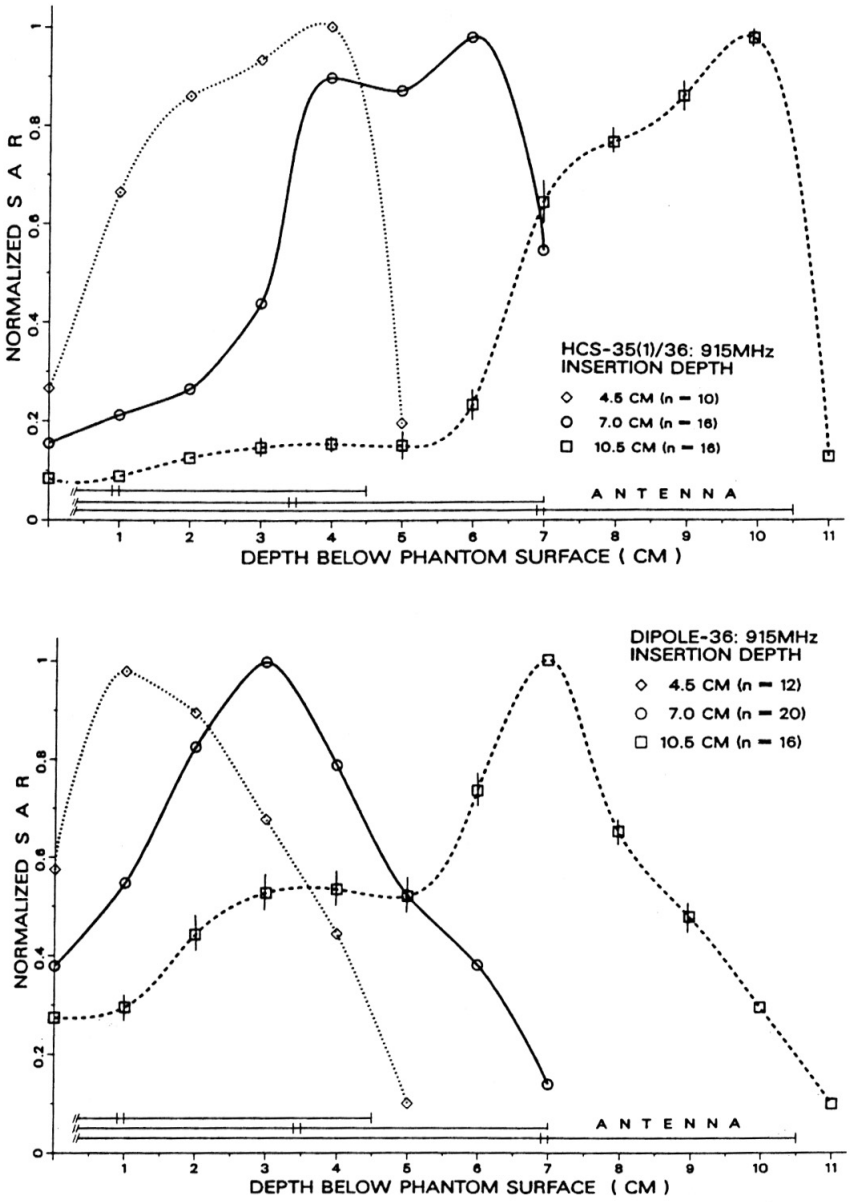

Fig. 4. (a) Power deposition profiles of HCS-35(1)/36 antennas measured parallel to the antenna axis at a radial distance of r = 5 mm from the antenna. Three different insertion depths were used: 4.5, 7.0, and 10.5 cm from the phantom surface to the antenna tip. Note the reproducibility of heating around the coil element which remained shifted toward the antenna tip independent of insertion depth. (b) Axial direction power deposition profiles at r = 5 mm for Dipole-36 antennas with total insertion depths in phantom ranging from 4.5 to 10.5 cm. Note the change in shape of the profiles obtained at different antenna insertion depths. Compare the profiles with those produced by the HCS-35(1)/36 antenna (Fig. 4a).

coil antennas was well-localized to the region surrounding the coil element, with little heating proximal to the antenna gap. The 50% HL could be varied from 3.5 to 5.2 cm by increasing the coil length from 3.0 to 5.0 cm (Table 1). Turn density had little effect on the 50% HL (Table 1), but did affect the shape of the peak shoulder of the profile significantly (Fig. 3). The peak depths were independent of coil length and turn density, and were generally located near the antenna tip. Within the range of parameters studied, dead lengths were essentially zero regardless of coil length or turn density (Table 1). These heating profiles were markedly different from those obtained using half-wavelength dipole antennas, where the temperature peak was located near the mid-depth junction and where there was a significant dead length along the antenna axis (Table 1).

The effects of antenna insertion depth on microwave induced heating profiles were considerably different between the HCS-35(1)/36 and Dipole-36 antennas (Table 2, Fig. 4a & 4b). Location of the temperature peak relative to the surface increased in direct correspondence with the increase in insertion depth of the HCS-35(1)/36

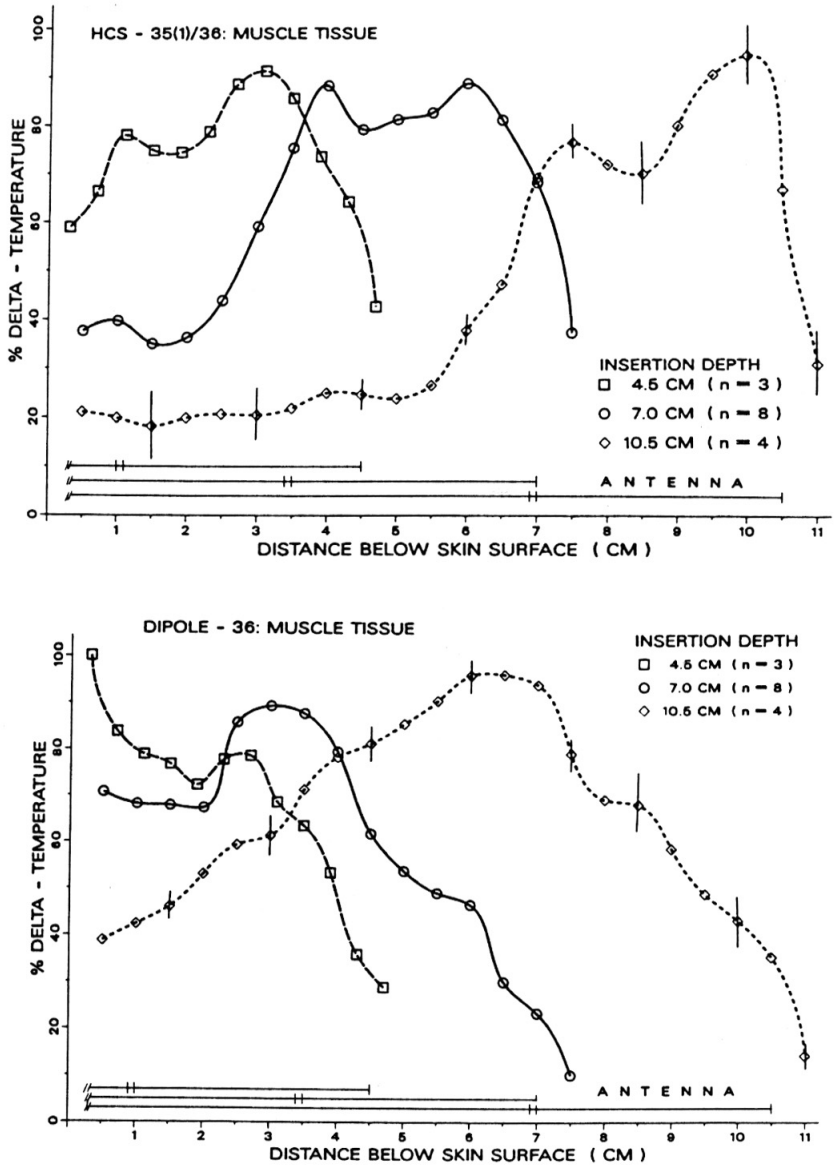

Fig. 5. (a) Axial direction thermal profiles at r = 5 mm for a single HCS-35(1)/36 antenna in canine muscle tissue *in vivo*. Peak temperatures of the profile with 4.5, 7.0, and 10.5 cm antenna insertion depths were 43.2 ± 1.3°C (average ± standard error of 3 sites), 43.0 ± 0.9°C (8 sites), and 43.1 ± 0.4°C (4 sites), respectively. For this comparative analysis of power deposition characteristics of different antennas in the same implant site, the *in vivo* data are plotted as % of the maximum Delta-T to eliminate complications from the different initial temperature distributions. Note the excellent localization of heating at depth, minimal dead length, and reproducibility of the heating pattern regardless of implant depth in muscle. (b) Corresponding axial thermal profiles for Dipole-36 antenna heating in the same *in vivo* muscle implant sites as used for Fig. 5a. Peak temperatures with 4.5, 7.0, and 10.5 cm insertion depths were 42.4 ± 0.7°C (3 implant sites), 43.3 ± 0.8°C (8 sites), and 43.0 ± 0.5°C (4 sites), respectively. Note the significant change of heating profile with different insertion depths and the excessive surface tissue heating observed with an insertion depth of 4.5 cm.

antennas. Overheating of surface tissues was not observed with antenna insertion depths in the range of 4.5–10.5 cm. Effective heating volumes were localized to the region around the coil element, with the peak near the antenna tip followed by a gentle sloping plateau along the helical coil length toward the antenna gap.

For Dipole-36 antennas, the power deposition profiles were strongly dependent upon antenna insertion depth and peak depths were no longer dependably centered about the antenna junction. Superficial tissue heating along the antenna feedline was more prominent for all insertion depths as compared to HCS antennas. Overheating of tissues near the antenna entrance point occurred only for short insertion depths less than a half-wavelength. Deeper insertions of the dipoles generally produced increases in both the 50% HL and dead length parameters, and a change in the shape of the r = 5 mm profiles.

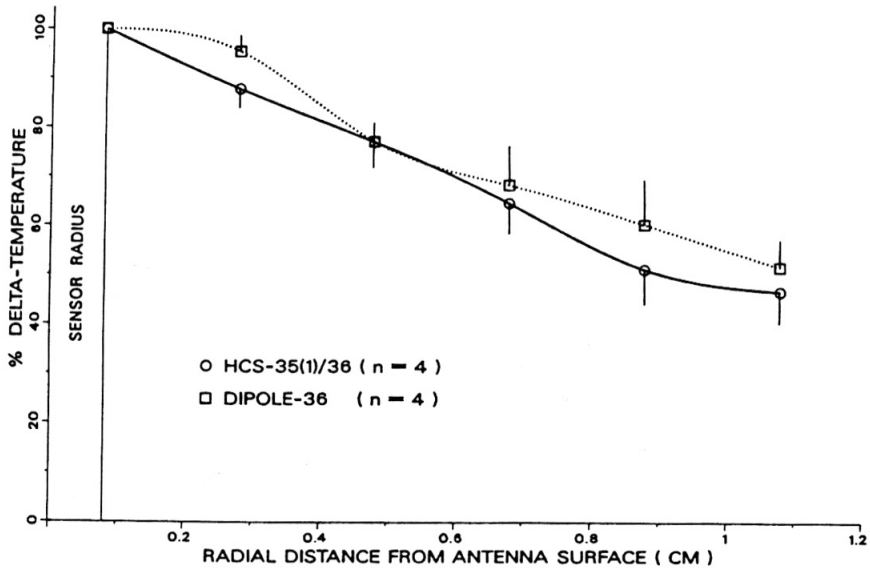

Fig. 6. Comparative radial thermal profiles of HCS-35(1)/36 and Dipole-36 antennas tested in the same muscle implant site *in vivo*. The antennas were inserted 7 cm deep, and profiles were obtained in the plane of the antenna gap, 3.5 cm below the skin surface.

In vivo experiments

From the phantom experiment results, the 3.5 cm long HCS-35(1)/36 antenna was selected as the most appropriate helical coil antenna for further comparative studies with the standard dipole antenna. Results of the *in vivo* comparative dosimetry of HCS-35(1)/36 and Dipole-36 antennas were generally in agreement with those predicted from phantom experiments. The thermal profiles of single HCS-35(1)/36 antennas in muscle were reproducible and well-localized around the helical coil elements, regardless of insertion depth (Fig. 5a). In contrast, the heating profiles of Dipole-36 antennas showed strong dependance on insertion depth and failure to heat tissue near the antenna tip effectively (Fig. 5b). With an insertion depth of 4.5 cm, the dipole antenna exhibited significant overheating of the area around the antenna entrance site with the surface tissue temperature becoming the distribution peak.

Thermal profiles recorded in the radial direction away from single microwave antennas and measured in the plane of the antenna gap showed similar temperature gradients for both the HCS-35(1)/36 and Dipole-36 antennas (Fig. 6). Heat penetration depths, described by the distance in the radial direction obtaining greater than 50% of the maximum delta-T at the antenna-catheter interface, were as long as 1 cm for both antenna types in the dog thigh muscle.

Heating patterns very similar to the single antenna r = 5 mm depth profiles shown in Figures 3–5 were obtained throughout the tissue volumes enclosed by four antenna square arrays of interstitial antennas. Figure 7a shows the temperature distributions measured along the central axes of 2 cm square arrays of four HCS 35(1)/36 and four DR-36 antennas, each inserted 7 cm deep in dog muscle. As in the single antenna studies, an effective shifting of the heated volume towards the antenna tips and low surface tissue temperatures were obtained at the center of HCS antenna arrays. Axial direction temperature distributions such as Figure 7a were measured along eight different catheters within the boundaries of 2 cm square arrays and the temperature rise data for each depth averaged to obtain a composite "array heating characteristic." This position averaged depth heating profile was further averaged between three different animal experiments to obtain the array heating characteristics shown in Figure 7b.

DISCUSSION

Interstitial microwave hyperthermia facilitates the localization of a therapeutic heating field to deep-seated target volumes within the body.[3,8,11] The effectiveness of interstitial hyperthermia depends upon the ability to predictably and reproducibly heat a given volume regardless of size, location, and microenvironment, while minimizing adverse effects to surrounding normal tissues.

Dipole microwave antennas[19–22] are commonly being used for interstitial hyperthermia treatments. Their application has been limited, however, because of their characteristic linearly polarized microwave radiation pattern. Heating profiles are strongly dependent upon insertion depth and physical antenna length;[4,13–15] if nonoptimal combinations are used, overheating of tissue at the antenna entrance site and unpredictable heat peaks along the antenna axis can result. Furthermore, the heating profile along the length of dipole antennas is essentially a circularly symmetric, gausian shaped distribution with a dramatic falloff of temperature in both directions

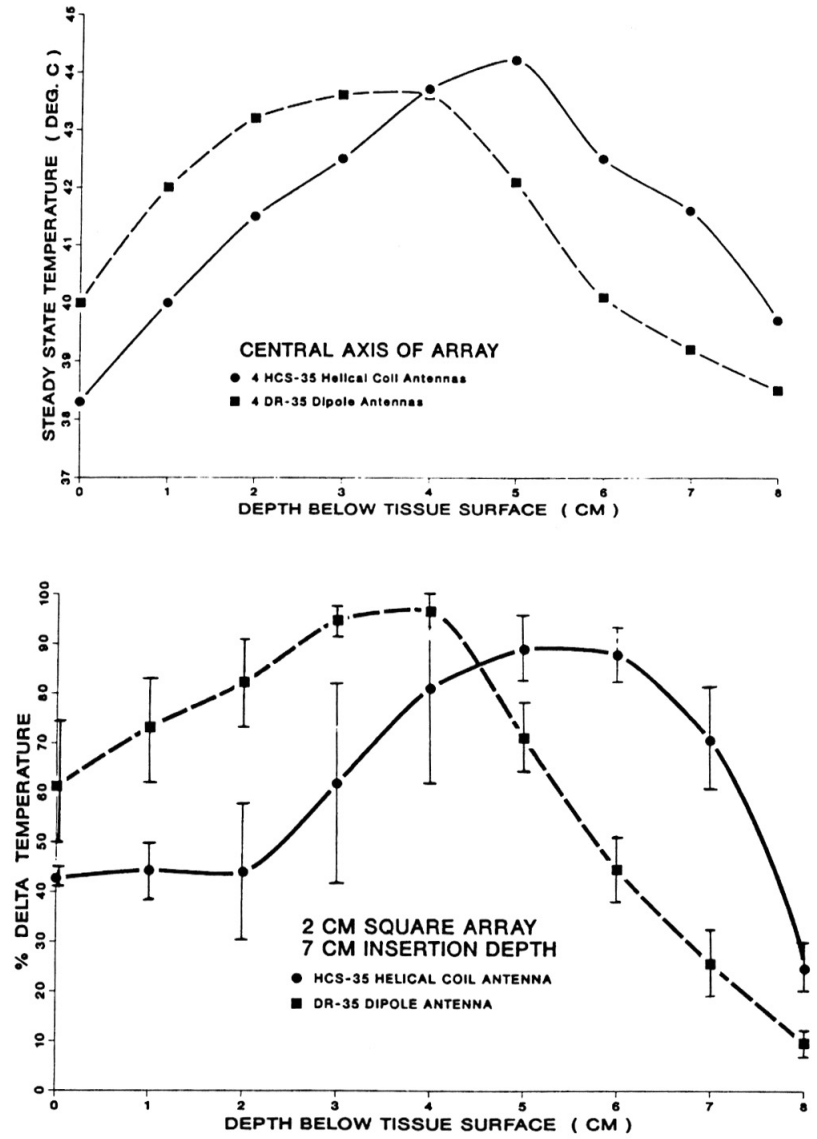

Fig. 7. (a) Temperature distributions with depth into tissue along a catheter located at the center of 2 cm square, four antenna arrays of HCS 35(1)/36 and DR-36 antennas in the same in vivo dog thigh muscle implant site; (b) Composite thermal profiles obtained by averaging the depth profiles from eight different locations within the 2 cm square arrays of Fig. 7a and combining the data from three animal experiments. The vertical bars represent the standard error of the mean of values from the three implant sites.

axially from a peak near the outer conductor discontinuity (junction). Tissue toward the antenna tip is generally not heated effectively,[7,8,14] so that significant over-implanting of the deep aspect of the tumor may be required. This could restrict applications of the treatment for certain tumors located near critical vascular or nervous tissues.

In an effort to improve the performance of implantable radiating antennas, several new designs and techniques have been introduced. Multijunction[8] and multinode[5] antennas have been used to expand the effective heating length for a given frequency. Although partially accomplishing this goal, the antennas still exhibit variable heating characteristics with different insertion depths, significant dead length, and multiple heat peaks along the antenna axis. Another technique for expanding the heating length has been proposed which uses a reciprocated motion system for linearly translating a dipole antenna during treatment.[9] Although this technique could potentially smooth out the axial heating pattern, it might be difficult to predict and control the overall heating field due to changes of power deposition pattern with variable antenna insertion depth. A variable diameter dipole antenna has been used to concentrate the heating current into larger diameter sections of the antenna which fit the implant catheter more tightly.[22] Although the antenna appears to provide more effective tip heating, the linearly polarized dipole still exhibits a signifi-

cant dependence of the heating pattern on insertion depth. A helical coil antenna structure has been reported previously for use in intracavitary heating at 300, 400, 650, and 915 MHz.[6] For this applicator, a 1.0 cm O.D. helix with 10 turns per 14 cm length and three interspaced copper rings was used to connect the feedline outer conductor to the distal end of the inner conductor without a discontinuity (gap). The temperature profiles in the axial direction were quite variable for the different conditions studied and showed strong dependence on both source frequency and insertion depth. Recently, two interstitial antenna designs have been reported with data indicating significant improvement in heating. Good tip heating characteristics are shown for the "sleeved coaxial slot radiator"[7] but no data are given regarding changes to the heating pattern of the lineally polarized antenna for different insertion depths. Finally, a miniature implantable "Helical microwave interstitial antenna" similar to that described in the present studies was reported by Wu.[23] As in the helical intracavitary antenna,[6] a coil structure was connected between the inner and outer conductors of the coaxial cable feedline. Single antenna phantom SAR patterns were shown which had improved tip heating relative to the linearly polarized "reference" antenna. This conclusion agreed with the results of the present study but no detail on heating at different insertion depths was given.

Previous work in our laboratory established the basic design parameters of an interstitial helical coil microwave antenna for use at 2450 MHz.[14] An extensive characterization of thermal distributions was performed in phantoms and animals to determine the effects of helical coil turn density and connection configuration of the coil to the coax feedline on the resultant heating profiles. A helical coil-separated type connection configuration with a 1 mm gap and 10 turns per 10 mm length coil element (HCS-10(1)/11) demonstrated a dramatic shift of the effectively heated volume toward the antenna tip and complete independence of heating on antenna insertion depth. Other combinations of parameters yielded a variety of different heating patterns ranging from distorted helical coil type patterns to essentially dipole antenna type heating patterns.

The present study extended this work, incorporating a similar antenna design for use at 915 MHz. Heating patterns of single helical coil antennas were characterized at several insertion depths in both phantom and in vivo muscle tissues to simulate various tumor treatment conditions. The localization of heat to the region surrounding the coil element, reproducibility of heating patterns with variable insertion depth, essentially zero dead length, and the reduced surface tissue heating were considered significant improvements over standard dipole antennas. These characteristics suggest that helical coil microwave antennas can increase the potential applications of interstitial microwave hyperthermia through improved heat localization, simplified treatment planning, and minimization of both treatment limiting surface heating and the requirement for over-implantation of the tumor volume deep margin.

REFERENCES

1. Chou, C., Chen, C., Guy, A., Luk, K.K.: Formulas for preparing phantom muscle tissue at various radiofrequencies. *Bioelectromagnetics* **5:** 435–441, 1984.
2. Cosset, J.M., Brule, J., Damia, E., Salama, M.: Low frequency contact and interstitial hyperthermia in association with brachytherapy. *Int. J. Radiat. Oncol. Biol. Phys.* **10:** 307–312, 1984.
3. Coughlin, C.T., Wong, T.Z., Strohbehn, J.W., Colacchhio, T.A., Sutton, J.E., Belch, R.Z., Douple, E.B.: Intraoperative interstitial microwave-induced hyperthermia and brachytherapy. *Int. J. Radiat. Oncol. Biol. Phys.* **11:** 1673–1676, 1985.
4. de Sieyes, D.C., Douple, E.B., Strohbehn, J.W., Trembly, B.S.: Some aspects of optimization of an invasive microwave antenna for local hyperthermia treatment of cancer. *Med. Phys.* **8:** 174–183, 1981.
5. Lee, D., O'Neill, M.J., Lam, K., Rostock, R., Lam, W.: A new design of microwave interstitial applicator for hyperthermia with improved treatment volume. *Int. J. Radiat. Oncol. Biol. Phys.* **12:** 2003–2008, 1986.
6. Li, D-J., Luk, K.H., Jiang, H-B., Chou, C-K., Hwang, G-Z.: Design and thermometry of an intracavitary microwave applicator suitable for treatment of some vaginal and rectal cancers. *Int. J. Radiat. Oncol. Biol. Phys.* **10:** 2155–2162, 1984.
7. Lin, J.C., Wang, Y.J.: Interstitial microwave antennas for thermal therapy. *Int. J. Hyperther.* **3**(1): 37–47, 1987.
8. Neyzari, A., Cheung, A.Y.: A review of brachyhyperthermia approaches for the treatment of cancer. *Endocurie. Hypertherm. Oncol.* **1:** 257–264, 1985.
9. Nohara, H., Hiraoka, M., Jo, S., Ono, K., Takahashi, M., Abe, M.: A microwave applicator for intracavitary hyperthermia. *Jpn. J. Clin. Radiol.* **29:** 1035–1039, 1984. (in Japanese)
10. Perez, C.A., Emami, B.: A review of current clinical experience with irradiation and hyperthermia. *Endocurie. Hypertherm. Oncol.* **1:** 265–277, 1985.
11. Roberts, D.W., Coughlin, C.T., Wong, T.Z., Fratkin, J.D., Douple, E.B., Strohbehn, J.W.: Interstitial hyperthermia and iridium brachytherapy in treatment of malignant glioma: A phase I clinical trial. *J. Neurosurg.* **64:** 581–587, 1986.
12. Salazar, O.M., Samaras, G.M., Eddy, H.A., Amin, P.P., Sewchand, W.S., Drzymala, R.E., Bajaja, K.G.: Neurobrachytherapy; a new frontier. *Endocurie. Hypertherm. Oncol.* **2:** S-3–S-15, 1986.
13. Samaras, G.M.: Intracranial microwave hyperthermia: heat induction and temperature control. *IEEE Trans. BME* **31:** 63–69, 1984.
14. Satoh, T., Stauffer, P.R.: Implantable helical coil microwave antenna for interstitial hyperthermia. *Int. J. Hyperthermia* (In press) 1988.
15. Sneed, P.K., Matsumoto, K., Stauffer, P.R., Fike, J.R., Smith, V., Gutin, P.H.: Interstitial microwave hyperther-

mia in a canine brain model. *Int. J. Radiat. Oncol. Biol. Phys.* **12:** 1887–1897, 1986.

16. Stauffer, P.R., Suen, S., Satoh, T., Fike, J.R.: Comparative thermal dosimetry of interstitial RF and microwave heating. *IEEE Proc. 8TH Annual Conference of Engr. Med. Biol. Soc.* 1986, pp. 1458–1462.
17. Stauffer, P.R., Suen, S., Satoh, T., Sneed, P.K., Fike, J.R.: Validity of an *in vivo* tissue model for comparative thermal dosimetry. *IEEE Proc. 9TH Annual Conference of Engr. Med. Biol. Soc.* 1987, pp. 997–999.
18. Stauffer, P.R., Suen, S.A., Satoh, T., Sneed, P.K., Fike, J.R., Phillips, T.L.: Comparative thermal dosimetry of interstitial microwave and radio frequency-LCF hyperthermia. *Int. J. Hyperther.* (In press) 1988.
19. Strohbehn, J.W., Bowers, E., Walsh, J., Douple, D.B.: An invasive microwave antenna for locally induced hyperthermia for cancer therapy. *J. Microwave Power* **14:** 181–186, 1979.
20. Taylor, L.S.: Electromagnetic syringe. *IEEE Trans. BME* **25:** 303–304, 1978.
21. Trembly, B.S., Strohbehn, J.W., King, R.W.P.: Practical embeded insulated antenna for hyperthermia. *Proc. 10th Northeast Bioeng. Conf.* 1982, pp. 105–108.
22. Turner, P.: Interstitial equal-phased arrays for hyperthermia. *IEEE Trans. Mic. Theory & Techniques* **34:** 572–578, 1986.
23. Wu, A., Watson, M.L., Sternick, E.S.: Performance characteristics of a helical microwave interstitial antenna for local hyperthermia. *Med. Phys.* **14**(2): Mar/Apr. 1987.